RESONANCE CHARACTERISTICS OF NON-UNIFORM WIDTH SQUARE RING ANTENNAS

S. Behera[*] and K. J. Vinoy

Microwave Laboratory, Department of Electrical Communication Engineering, Indian Institute of Science, Bangalore 560012, India

Abstract—This paper presents a study of the effects of line width on the resonance frequency and bandwidth of a microstrip square-ring antenna at its primary resonance frequency. Although such ring antennas operating in TM_{11} mode are smaller than regular patch antennas, they are not explored much as they are considered to have poor bandwidth and efficiency at this mode. We have used a transmission line model to study their input characteristics and found that a non-uniform width ring antenna has significantly better (nearly double) bandwidth and radiation efficiency than a uniform width square ring antenna. Extensive simulations were done and a prototype non-uniform width square ring antenna is fabricated and tested to verify these results.

1. INTRODUCTION

Microstrip ring antennas have received much attention because of their low profile and light weight, meeting the demand of miniaturized antennas for small portable wireless applications [1–11]. This antenna can be considered as a microstrip patch antenna, with a significant portion of the conductor from its middle removed. The area of this removed portion provides a new parameter to control its resonance and input characteristics. The resonant behavior of microstrip circular-ring geometries was studied by Mink in 1980's [12]. It was observed that for an annular ring resonator, the resonance frequency of the lowest order mode can be much lower than a circular microstrip patch antenna of the same size. A similar effect is true with microstrip square ring antennas [13]. Microstrip ring antennas of various shapes are studied in different contexts [1, 2, 14–21].

We can designate the modes of the microstrip ring antennas by using the patch antenna as the reference. As in patches, the radiation behavior of the annular-ring antenna can be obtained by replacing its peripheries with magnetic walls. If the electromagnetic fields are assumed to be confined to the dielectric volume between the perfectly conducting ground plane and the radiating conductor, the fields may be shown to be transverse magnetic (TM) to the boresight (z) direction. It has been shown that the ring structure is a good resonator (with very little radiation) for TM_{1m} modes (m odd), and a good radiator for TM_{1m} modes (m even) [14, 22].

Various analyses have shown that the TM_{12} mode is the best mode of microstrip annular-ring for antenna applications, while the TM_{11} mode having a high Q-factor, is best reserved for resonator applications [23]. This shows that microstrip ring geometries have very narrow bandwidth at the primary mode than similar sized regular patch antennas [16, 21]. However feed structures can affect the quality factor of resonators and several feeding mechanisms have been attempted to excite microstrip ring geometries for antenna applications. Yet in most simple feed configurations, these antennas have low bandwidth and poor efficiency in the primary mode (TM_{11}).

In this paper we investigate the effects of non-uniform width geometries in the resonance behavior of square ring antennas. A transmission line model is developed to understand the behavior of these antennas. The simulation study of these antennas is carried out using commercial software program Zeland IE3D, based on method of moments (MoM). The similarity in the current distributions of various antennas confirms that all these operate in the same mode. Selected prototype antennas are fabricated and characterized using a vector network analyzer.

2. SQUARE RING ANTENNA AND ITS DESIGN

This group has recently proposed an out of plane capacitive feed arrangement for the microstrip ring antenna to use this for multi-frequency applications [24]. The antenna configuration in the present design has two dielectric layers. The dielectric layer at the bottom has a feed microstrip transmission line patterned on one side of this and copper ground on the other side. The top dielectric layer has a radiating ring on the outer side. The schematic of the antenna configuration is shown in Fig. 1.

As one could imagine, several parameters could be varied to arrive at an optimum antenna design. These include the dimensions (l_s, w_s) of the coupling strip attached to the transmission line. The mean
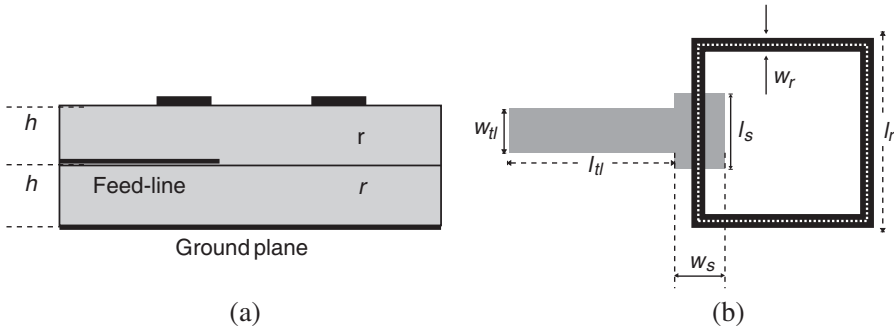
Figure 1. Geometry of the ring antenna.

perimeter of the ring is considered very critical in deciding its primary resonance frequency, especially for small ring widths (w_r). The design expression for ring antennas available in the literature [14] can be used to calculate the resonance frequency:

$$f_r = \frac{c}{4\left(l_r - w_r\right)\sqrt{\varepsilon_{eff}}} \tag{1}$$

where ε_{eff} is the effective permittivity of this multilayer microstrip structure for a line of width w_r (same as that of the ring) and l_r the outer length of perimeter of the square ring. For good accuracy, the effective line width of the microstrip line can be determined from [25]

$$w_{eff} = w_r + \frac{2h}{\pi}\ln\left[17.08\left(\frac{w_r}{2h} - 0.92\right)\right] \tag{2}$$

3. ANALYTICAL AND SIMULATION STUDIES

3.1. Transmission Line Model

In this section we first develop a lossy transmission line model for the analysis of the uniform width ring antenna and later extend this for non-uniform width ring geometries. Based on the symmetry of the geometry, an isolated ring can be divided into two transmission lines of equal length connected in parallel (Fig. 2). If the widths of all segments of the square ring are identical, all corners are equidistant. Therefore it is safe to assume that the corners of the ring have negligible effect on the input impedance as these are $\lambda/4$ apart. Although ends of these two sections are connected together to form the ring, we consider these to be open circuited at port 2 due to symmetry of the antenna geometry.
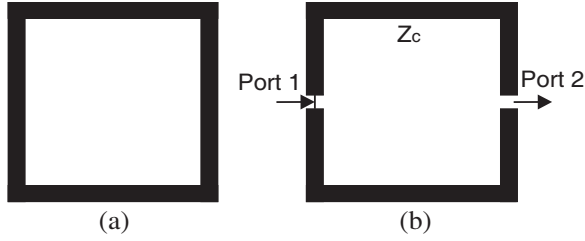
Figure 2. (a) An isolated ring geometry and (b) its equivalent two-port network.

Using the transmission line theory, the input impedance of each of these transmission line segments can be obtained as

$$Z_{\text{in}} = -jZ_c \cot \beta l \tag{3}$$

where Z_c is the characteristic impedance of the microstrip line with uniform width and β the corresponding propagation constant.

We can define the electrical length of each section of the ring structure as:

$$\beta l = \frac{\omega}{v_p} l \tag{4}$$

where v_p is the phase velocity. It may be noted that near the resonance frequency ω_0, we can replace $\omega = \omega_0 + \Delta\omega$, with $\Delta\omega$ being very small. Recalling that for a uniform width ring, $l = \lambda_g/2$ at the resonance, Equation (4) can be written as,

$$\beta l = \frac{\omega_0 l}{v_p} + \frac{\Delta\omega l}{v_p} = \pi + \frac{\Delta\omega\pi}{\omega_0} \tag{5}$$

The above analysis approach can be extended for ring geometries with non-uniform width. As in the previous case, the isolated non-uniform width ring is divided into two transmission line segments as shown in Fig. 3. Each of these parallel open-circuited sections can be considered as a stepped impedance resonator or non-uniform transmission line resonator.

From Fig. 3(b), we can obtain the input impedance at the end A as [22]

$$
\begin{aligned}
Z_{\text{in}} &= Z_2 \frac{Z_{\text{in}2} + jZ_2 \tan\theta_2}{Z_2 + jZ_{\text{in}2} \tan\theta_2} \\
&= jZ_2 \frac{\left\{ 2\left(1+K^2\right)\tan\theta_1 \tan\theta_2 - K\left(1-\tan^2\theta_1\right)\left(1-\tan^2\theta_2\right)\right\}}{2\left(\tan\theta_2 + K\tan\theta_1\right)\left(K - \tan\theta_1 \tan\theta_2\right)}
\end{aligned} \tag{6}
$$
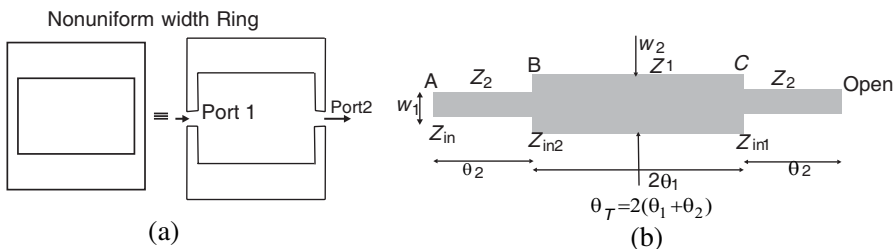
Figure 3. (a) Non-uniform width ring geometry and its equivalent two-port network. (b) Transmission line section of (a).
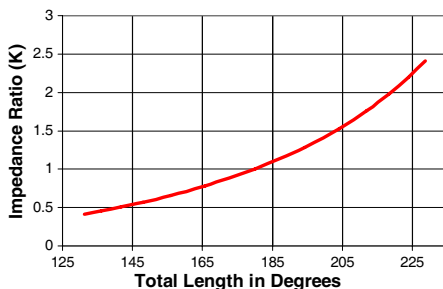
Figure 4. Resonant condition of the stepped impedance resonator.

where the impedance ratio $K = Z_2/Z_1$. For the ring, two such lines are connected in parallel. The admittance of each can therefore be expressed as

$$Y_{\text{in}} = jY_2 \frac{2\left(\tan\theta_2 + K\tan\theta_1\right)\left(K - \tan\theta_1\tan\theta_2\right)}{\left\{K\left(1 - \tan^2\theta_1\right)\left(1 - \tan^2\theta_2\right) - 2\left(1 + K^2\right)\tan\theta_1\tan\theta_2\right\}} \quad (7)$$

Since Y_{in} is purely imaginary, the condition for resonance ($Y_{\text{in}} = 0$) leads to,

$$K = \tan\theta_1 \tan\theta_2 \quad (8)$$

It may be noted that only when $K = 1$ (uniform width) the total electrical length will be π. It is interesting to note that the electrical length varies with K and is plotted in Fig. 4. A similar trend can therefore be expected for the ring antenna as well.

The feed microstrip line has a rectangular strip known as coupling strip, placed at the end of the line to couple energy to the radiating ring. This discontinuity in a feeding microstrip transmission line has been designed to enhance coupling of energy to the radiating ring. The input impedance of the ring antenna is

$$Z_{\text{ant}} = \left(Z_{\text{cap}} + Z_{\text{in}}\right) \times g \quad (9)$$

where Z_{cap} is the series capacitance between the ring and the feed strip and g the impedance normalization factor. Furthermore, the effect of loss can be incorporated by replacing ω_0 in Equations (6) with a complex effective resonance frequency [26–28] as:

$$\omega_0 \leftarrow \omega_0 \left(1 + \frac{j}{2Q} \right) \tag{10}$$

These may be substituted in (9) to determine the full expression for the input impedance of the antenna.

3.2. Studies on Changing Ring Width

First, the square ring antennas of uniform width are studied by expanding the ring width uniformly on all sides. Several antenna geometries have been simulated using IE3D to study the effects on various antenna performance parameters. These simulated results are given in the Table 1. It is established that an increase in width of the ring the resonance frequency is slightly shifted to a lower frequency. As the width of ring antenna is increased, the effective permittivity increases, which causes the resonance frequency to decrease. As noted earlier the guided wavelength λ_g is approximately equal to the mean perimeter of the antenna at the resonance frequency.

However, it has been found from Table 2 that by increasing the width of two sides of the square ring parallel to the feed transmission line (Fig. 3(a)) the resonance frequency is shifted to higher frequencies. For a meaningful comparison the mean perimeter is kept unchanged. Even though all sides have the same physical length, their electrical lengths are not equal as the widths are different. Based on Fig. 4, it

Table 1. The simulated performance of square ring antenna as its width is varied. The mean perimeter (*MP*) of the antenna is kept constant at 90.8 mm.

w_r (mm)	ε_{reff}	f_r (GHz)	BW (MHz)	% BW	Gain (dBi)
1	1.8848	2.469	16.4	0.664	5.31
2	1.9228	2.458	20.6	0.838	5.6
3	1.9543	2.4502	24.2	0.988	5.78
4	1.9830	2.4442	27.6	1.13	5.91
5	2.0074	2.443	29.4	1.203	6.05
6	2.0287	2.437	33.2	1.362	6.12
7	2.0477	2.431	36.9	1.518	6.1

Table 2. Summary of the simulated performance of the ring antenna as the width of only two sides are varied. Other parameters: $w_1 = 1\,\text{mm}$, mean perimeter $(MP) = 90.8\,\text{mm}$. The dimensions of feed strip is adjusted in each case for a good impedance match.

W_2 (mm)	f_r (GHz)	S_{11} (dB)	BW (MHz)	% BW $= \frac{\text{BW}}{f_r} \times 100$	Total Q_T	Gain (dBi)
1	2.469	-42.3	16.4	0.664	106.5	5.31
2	2.662	-30.7	25.6	0.962	73.5	5.81
3	2.799	-27	31.8	1.136	62.25	6.01
4	2.906	-43	43.6	1.50	47.14	6.1
5	2.998	-43.9	53.8	1.795	39.4	6
6	3.08	-21.8	57.6	1.871	37.8	6.25
7	3.15	-24.3	75.2	2.226	31.76	6.27

can be concluded that the mean perimeter of the antenna is less than a guided wavelength at its resonance.

Furthermore, this modification causes the bandwidth to increase significantly. It is interesting to note that the bandwidth improvement in this case is twice as much of the uniform width antenna with 7 mm. The radiation efficiency and gain are also marginally better in this configuration.

In order to systematically observe the effects of changing the relative lengths of various segments of the ring antenna, we investigated antenna configurations by changing the aspect ratio of the geometry. This causes θ_1 and θ_2 to differ shown in Fig. 3(b). As an example, two extreme cases are shown in Fig. 5. Physical dimensions and the performances of various geometries considered in this study are presented in Table 3. In the table, $X = l_{r2} - w_1$, and $Y = l_{r1} - w_2$. The aspect Ratio of these geometries is defined as $AR = X/Y$. It may be reiterated that the mean perimeter $MP = 2(X+Y)$ is kept constant in this study.

Based on these studies it is observed that, the antenna with $AR = 1$ is best suited for use in practical applications as it has hold good bandwidth and good gain at the resonance frequency. However the aspect ratio affects the resonance frequency of the antenna geometry. Therefore these simulation results conclude that non-uniform width ring antennas with unity aspect ratio $= 1$, would be best suited for antennas. Since the resonance condition for this antenna is similar to that of the uniform width ring, we may conclude that all these antennas operate at the same mode. The improvement in the radiation efficiency and gain of these antennas can therefore be explained based on their current distributions.
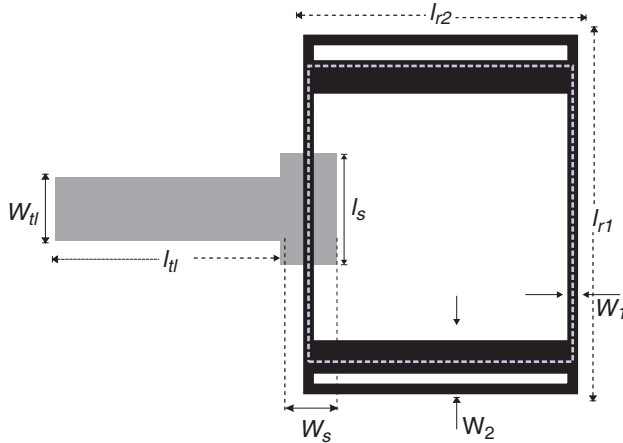
Figure 5. Geometry of the non-uniform width ring antenna.

Table 3. Geometrical Parameters and results for MSRAs for various aspect ratios.

l_{r1} (mm)	l_{r2} (mm)	X (mm)	Y (mm)	AR	f_r (GHz)	BW (MHz)	Gain (dBi)
32.7	20.7	19.7	25.7	0.7663	3.258	71.2	2.71
31.7	21.7	20.7	24.7	0.8381	3.23	75.2	2.79
30.7	22.7	21.7	23.7	0.915	3.195	75.6	3.08
29.7	23.7	22.7	22.7	1	3.15	75.2	6.27
28.7	24.7	23.7	21.7	1.092	3.105	73	6.23
27.7	25.7	24.7	20.7	1.192	3.06	70	5.2
26.7	26.7	25.7	19.7	1.304	3.005	67.2	5.2

3.3. Discussion of Radiation Modes and Currents

The radiation mode can be determined by comparing the currents in these antennas with those on a patch antenna. The simulated current distributions of various antenna geometries at their first resonances are included in Fig. 6. Directions of currents on the antenna conductor (as determined from numerical simulations) are shown in each case. It is widely known that the dominant mode in a circular patch in Fig. 6(a) is TM_{11}. Since the current distributions in all these cases are similar, we could state that all these antennas have primary resonance in the TM_{11} mode. However the resonant dimension of the ring geometry is
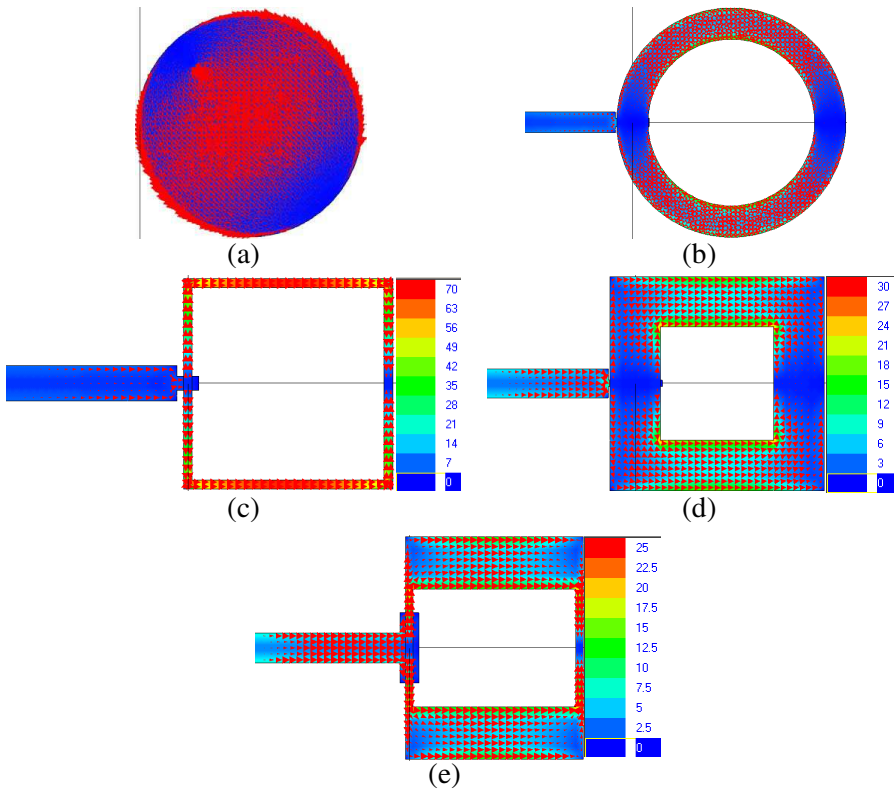
Figure 6. Simulated current distribution at the primary resonance of various antennas. (a) Patch antenna at resonance. (b) Narrow annular ring at resonance. (c) Narrow square ring at resonance. (d) Wide uniform ring at resonance. (e) Non-uniform width ring at resonance.

the mean perimeter while that for the patch is based on its radius. It may be recalled that the resonance of the square ring of uniform width is also determined by the perimeter.

The currents in the antenna geometry can be used to explain the resonance behavior of these antennas. For example, we observe that magnetic current ring sources for the narrow annular ring in Fig. 6(b) are of opposite polarity and are very close to each other for the TM_{11} mode. The polarity of these magnetic currents on the annular ring can be easily deduced from the fringing field near the edge of the patch. The radiated fields from the inner and outer edges of the annular ring of narrow width ring will therefore interfere resulting in a narrow bandwidth and poor radiation efficiency for such antennas.

It is because of this that the TM_{11} mode is usually considered a poor radiation mode for annular ring antennas.

The simulated current distribution of uniform width of $1\,mm$ square ring antenna is shown in Fig. 6(c). It has been observed that, the resonance frequency mode of this square ring antenna is similar to that of the narrow annular ring antenna. Hence one could state that the dominant mode of square ring antennas is TM_{11}. Similarly, the current distribution of the square ring antenna of uniform $7\,mm$ width is shown in Fig. 6(d). The behavior of current distribution is similar to that of the previous case, but Q of the antenna is reduced as the edge magnetic currents are spatially separated in this case. The current distribution of the non-uniform width square ring antenna shown in Fig. 6(e) is also similar to this. However, comparing the maximum values of currents from the sidebars in (d) and (e), one can infer the lower Q for the latter geometry. Hence the bandwidth in this case is more than in the previous cases.

4. EXPERIMENTAL VALIDATION

The prototype antenna is fabricated using standard printed circuit fabrication techniques and the photograph of the fabricated antenna is shown in the Fig. 7. The feed transmission line is hidden inside the dielectric layers. The antenna is characterized for its input characteristics using a vector network analyzer. The simulated, measured and analytical (using Eq. (9)) S_{11} of the non-uniform width square-ring microstrip antenna is shown in Fig. 8. As may be noted from the summary in Table 4, these are in good agreement.
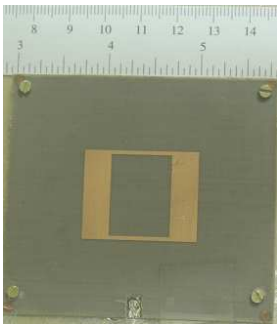
Figure 7. Photograph of a fabricated non-uniform width square ring antenna.
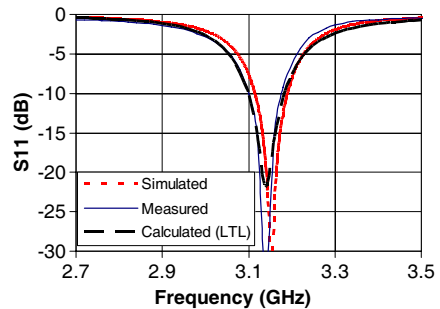
Figure 8. S_{11} characteristics of fabricated non-uniform width square ring antenna.

Table 4. Geometrical parameters and experimental results for the fabricated prototype antenna with a mean perimeter (MP) of 90.8 mm.

Parameters		Uniform width Ring Antenna	Non-uniform width Ring Antenna
Ring Width	W_1 (mm)	7	1
	W_2 (mm)	7	7
Feed Strip	Width w_s (mm)	7.5	2.5
	Length l_s (mm)	0.9	7.4
Resonance frequency (GHz)	Simulated	2.431	3.15
	Measured	2.431	3.152
Bandwidth (MHz)	Simulated	36.4	75.2
	Measured	36	75.5
Gain (dB)	Simulated	6.15	6.27
	Measured	4.8	5.4
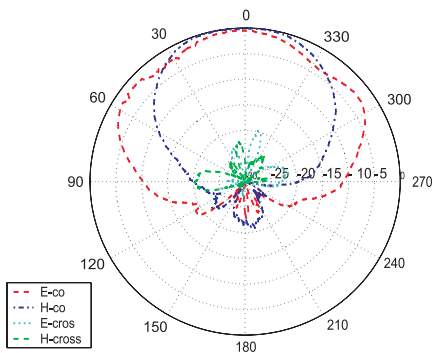
Figure 9. Measured radiation patterns of the non-uniform width ring antenna at 3.151 GHz.
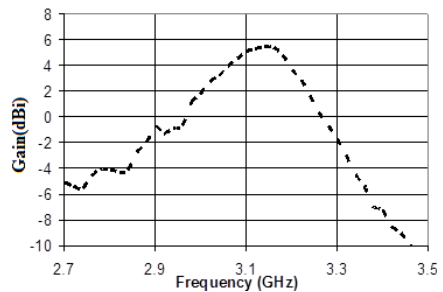
Figure 10. Measured gain of the antenna.

The radiation patterns (co- and cross-polarization) of these ring antennas are measured in a shielded anechoic chamber and plotted at the corresponding resonance frequency. The nature of radiation patterns shown in Fig. 9 confirm TM_{11} mode in the square ring antenna with non-uniform width antenna. This also indicates that

corner radiations do not adversely contribute to the radiations from the antenna. Therefore this geometry can be used as a narrowband antenna. The measured gain of this antenna is shown in Fig. 10. It is also possible to modify this geometry further to make dual frequency antennas [24, 29]. Therefore from the antenna perspective, the resonance characteristics of the non-uniform width square ring geometry appear to be much more useful than those of uniform width annular or square ring geometries.

5. SUMMARY

This paper demonstrates that the resonance characteristics of a non-uniform width geometry are somewhat different from uniform width annular or square ring geometries. Although all considered geometries have the primary resonance in the TM_{11} mode, and the loop currents of these geometries determine their resonances, the non-uniform width geometry stands out, particularly from an antenna perspective. The resulting antenna has significantly better radiation characteristics (bandwidth and efficiency) than a uniform width ring in TM_{11} mode, and is much smaller in size than a rectangular patch antenna. A transmission line model is used to explain the input characteristics of this antenna. These results are further validated with experimental results.

REFERENCES

1. Nurie, N. S. and R. J. Langley, "Input impedance of concentric ring microstrip antennas for dual-frequency band operation including surface wave coupling," *IEE Proceedings H Microwaves, Antennas and Propagation*, Vol. 137, No. 6, 331–336, Dec. 1990.

2. Garg, R. and V. S. Reddy, "Edge feeding of microstrip ring antennas," *IEEE Trans. on Antennas and Propagation*, Vol. 51, No. 8, 1941–1946, Aug. 2003.

3. Mayhew-Ridgers, G., J. W. Odendaal, and J. Joubert, "Single-layer capacitive feed for wideband probe-fed microstrip antenna elements," *IEEE Trans. on Antennas and Propagation*, Vol. 51, No. 6, 1405–1407, Jun. 2003.

4. Ramirez, R. R., F. De Flaviis, and N. G. Alexopoulos, "Single-feed circularly polarized microstrip ring antenna and arrays," *IEEE Trans. on Antennas and Propagation*, Vol. 48, No. 7, 1040–1047, Jul. 2000.

5. Kokotoff, D. M., J. T Aberle, and R. B. Waterhouse, "Rigorous

analysis of probe-fed printed annular ring antennas," *IEEE Trans. on Antennas and Propagation*, Vol. 47, No. 2, 384–388, Feb. 1999.

6. Latif, S. I. and L. Shafai, "Investigation on probe-fed open ring microstrip antenna for miniaturization," *Microwave and Optical Technology Letters (MOTL)*, Vol. 48, No. 11, 2175–2179, Nov. 2006.

7. Chen, W.-S., C.-K. Wu, and K. L. Wong, "Square-ring microstrip antenna with a cross strip for compact circular polarization operation," *IEEE Trans. on Antennas and Propagation*, Vol. 47, No. 10, 1566–1568, Oct. 1999.

8. Sultan, M. A., "The mode features of an ideal-gap open-ring microstrip antenna," *IEEE Trans. on Antennas and Propagation*, Vol. 37, No. 2, 137–142, Feb. 1989.

9. Wu, Y. S. and F. J. Rosenbaum, "Mode chart for microstrip ring resonator (short Paper)," *IEEE Trans. on Microwave Theory and Techniques*, 487–489, Jul. 1973.

10. Liu, J.-C., B.-H. Zeng, L. Badjie, S. Drammeh, S.-S. Bar, T.-F. Hung, and D.-C. Chang, "Single-feed circularly polarized aperture-coupled stack antenna with dual-mode square loop radiator," *IEEE Antennas and Wireless Propagation Letters*, Vol. 9, 887–890, 2010.

11. Rezaiesarlak, R., F. Hodjat Kashani, and E. Mehrshahi, "Analysis of capacitively coupled microstrip-ring resonator based on spectral domain method," *Progress In Electromagnetics Research Letters*, Vol. 3, 25–33, 2008.

12. Mink, J. W., "Circular ring microstrip antenna elements," *IEEE Antennas and Propagation Society Int. Symp. Digest*, 605–608, 1980.

13. Bafrooei, P. M. and L. Shafai, "Characteristics of single- and double-layer microstrip square-ring antennas," *IEEE Trans. on Antennas and Propagation*, Vol. 47, No. 10, 1633–1639, Oct. 1999.

14. Garg, R., P. Bhartia, I. J. Bhal, and A. Ittipiboon, *Microstrip Antenna Design Handbook*, Artech House, Boston, 2001.

15. Mayhew-Ridgers, G., J. W. Odendaal, and J. Joubert, "New feeding mechanism for annular-ring microstrip antenna," *Electronics Letters*, Vol. 36, No. 7, 605–606, Mar. 30, 2000.

16. Row, J. S., "Design of square-ring microstrip antenna for circular polarization," *Electronics Letters*, Vol. 40, No. 2, Jan. 22, 2004.

17. Ansari, J. A., R. B. Ram, and P. Singh, "Analysis of a gap-coupled stacked annular-ring microstrip antenna," *Progress In Electromagnetics Research B*, Vol. 4, 147–158, 2008.

18. Ren, Y. J. and K. Chang, "An annular ring antenna for UBW communications,," *IEEE Antennas and Wireless Propagation Letters*, Vol. 5, No. 1, 274–276, 2006.

19. Mellah, S., M. Drissi, J. M. Floch, and J. Citerne, "Theoritical and Experimental investigation of smooth and discrete microstrip ring antennas," *IEEE Antennas and Propagation Society Intern. Symp.*, Vol. 4, 2196–2199, 1992.

20. Latif, S. I. and L. Shafai "Dual-layer square-ring (DLSRA) for circular polarization," *IEEE Antennas and Propagation Society Intern. Symp.*, Vol. 2A, 525–528, 2005.

21. Chen, S. H., J. S. Row, and C. Y. D. Sim, "Single-feed square-ring patch antenna with dual-frequency operation," *Microwave and Optical Technology Letters*, Vol. 49, 991–994, 2007.

22. James, J. R. and P. S. Hall, *Handbook of Microstrip Antennas*, Vol. 1, Peter Peregrinus Ltd., London, 1989.

23. Chew, W. C., "A broad-band annular-ring microstrip antennas," *IEEE Trans. on Antennas and Propagation*, Vol. 30, No. 5, 918–922, Sep. 1982.

24. Pal, A., S. Behera, and K. J. Vinoy, "Design of multi-frequency microstrip antennas using multiple rings," *IET Microwaves Antennas & Propagation*, Vol. 3, 77–84, 2009.

25. James, J. R., et al., "Some recent developments in microstrip antenna design," *IEEE Trans. on Antennas and Propagation*, Vol. 29, 124–128, Jan. 1981.

26. Pozar, D. M. and B. Kaufman, "Increasing the bandwidth of a microstrip antenna by proximity coupling," *IEE Electronics Letters*, Vol. 3, No. 8, 368–369, Apr. 1987.

27. Pozar, D. M., *Microwave Engineering*, John Wiley & Sons. Inc., 2005.

28. Cheng, D., "Compact multi-band multi-port antenna," US Patent 7289064, Oct. 30, 2007.

29. Behera, S. and K. J. Vinoy, "Microstrip square ring antenna for dual-band operation," *Progress In Electromagnetics Research*, Vol. 93, 41–56, 2009.